JOURNAL OF PLANKTON RESEARCH | VOLUME 29 | NUMBER 9 | PAGES 803–821 | 2007

Asynchronous vertical migration and bimodal distribution of motile phytoplankton

DAVID K. RALSTON[1]*, DENNIS J. MCGILLICUDDY, JR.[1] AND DAVID W. TOWNSEND[2]

[1]APPLIED OCEAN PHYSICS AND ENGINEERING, MS #12, WOODS HOLE OCEANOGRAPHIC INSTITUTION, WOODS HOLE, MA 02543, USA AND [2]SCHOOL OF MARINE SCIENCES, UNIVERSITY OF MAINE, ORONO, ME 04469, USA

*CORRESPONDING AUTHOR: dralston@whoi.edu

Received December 21, 2006; accepted in principle March 30, 2007; accepted for publication July 30, 2007; published online August 7, 2007

Communicating editor: K.J. Flynn

Some motile phytoplankton have the capability to exploit deep sources of nutrients in a vertical migration cycle: photosynthesis in the near-surface layer, transit to depth, uptake of the limiting nutrient and transit back to the surface layer. If all four steps can be completed within 24 h, then migrations can be synchronized to the day/night cycle to maximize photosynthetic efficiency. Alternatively, if physiological, behavioral or environmental factors make it impossible for the cycle to be completed in 24 h, then migration may be asynchronous. Many observations of phytoplankton reveal bimodal vertical distributions of organisms, with maxima near the surface and the nutricline. We demonstrate how bimodal vertical distributions of phytoplankton may be symptomatic of asynchronous vertical migration using a Lagrangian Ensemble numerical model. We simulate vertical migration of the dinoflagellate Alexandrium fundyense in conditions similar to those in the Gulf of Maine, where bimodal distributions of A. fundyense have been observed. Migration is regulated by internal nutritional state—organisms swim down toward the nitracline when depleted of nitrogen, and return to the surface after nutrient uptake. We test the sensitivity of the results to growth rate, nitrogen uptake rate and swimming speed, and find that organism distributions can be bimodal or unimodal depending on conditions. Finally, we develop an analytical estimate for population distribution based on organism characteristics and nutricline depth.

INTRODUCTION

An important adaptation of many dinoflagellates is the ability to migrate vertically in the water column, whether to retrieve subsurface nutrients (Eppley *et al.*, 1968; Cullen and Horrigan, 1981; Heaney and Eppley, 1981; Cullen, 1985; MacIntyre *et al.*, 1997; Fauchot *et al.*, 2005a), or to avoid high irradiance (Eppley *et al.*, 1968; Anderson and Stolzenbach, 1985; Ault, 2000; Fauchot *et al.*, 2005a) or energetic turbulence (Smayda, 1997; Peters and Marrasé, 2000; Sullivan *et al.*, 2003) near the surface. The mobility to access deep pools of nutrients or to adjust for optimal irradiance offers dinoflagellates potential ecological advantages over passive organisms, and internal accumulations of nutrients and carbohydrates permit flexibility to transition between growth and nutrient uptake phases depending on vertical position (Cullen, 1985; Flynn and Fasham, 2002). Vertical migration depends on a complex optimization based on the vertical distributions of light and nutrients as well as the nutritional state of the organisms, although the physiological details remain poorly defined (Kamykowski, 1995). Interspecies differences among dinoflagellates can lead to very different vertical migration strategies, and different cell distributions in the water column (Cullen, 1985).

Dinoflagellate species of the genus *Alexandrium* have been observed or inferred to migrate vertically in both field and laboratory settings (Anderson and Stolzenbach,

doi:10.1093/plankt/fbm061, available online at www.plankt.oxfordjournals.org

© The Author 2007. Published by Oxford University Press. All rights reserved. For permissions, please email: journals.permissions@oxfordjournals.org

1985; Rasmussen and Richardson, 1989; MacIntyre *et al.*, 1997; Fauchot *et al.*, 2005a). *Alexandrium* species are of particular interest because some produce saxitoxins that can accumulate in the tissues of filter feeders and lead to outbreaks of paralytic shellfish poisoning (PSP). Toxic *Alexandrium* sp. blooms are common in the Gulf of Maine and coastal New England (Anderson *et al.*, 1994), but have been reported globally (Glibert *et al.*, 2005). Understanding the physical and biological factors that influence these blooms is important for public health, economic and ecological considerations. Here, we focus on the dominant species responsible for PSP in the Gulf of Maine, *A. fundyense*. Note that we consider *A. fundyense* and *A. tamarense* to be varieties of the same species (Anderson *et al.*, 1994).

The spatial distribution of *A. fundyense* blooms in the Gulf of Maine can be quite variable, with patchy concentrations of cells that depend on the coastal currents, freshwater plumes, wind direction and cyst bed locations (Anderson *et al.*, 2005). Vertical distributions of cells in the water column are also variable, with both surface and subsurface cell concentration maxima reported for *A. fundyense* (Townsend *et al.*, 2001, 2005a) and *A. tamarense* (Holligan *et al.*, 1984; Anderson and Stolzenbach, 1985; Franks and Anderson, 1992). Subsurface maxima often correspond with the bottom of the pycnocline and with the top of the nitracline, at a sharp gradient in dissolved inorganic nitrogen (DIN) concentration. Subsurface maxima at the nitracline have been reported for *Alexandrium* sp. (Sullivan *et al.*, 2003; Fauchot *et al.*, 2005a) as well as for other dinoflagellate species (Eppley *et al.*, 1968; Blasco, 1978; Cullen and Horrigan, 1981; Cullen *et al.*, 1983; Passow, 1991). In some instances, elevated cell populations have been found simultaneously at the surface and the nitracline (Holligan *et al.*, 1984; Townsend *et al.*, 2001). Three examples of *A. fundyense* concentration profiles with bimodal distributions are taken from the Gulf of Maine during late spring/early summer 2000 and 2001, and are plotted along with inorganic nitrogen concentration (Fig. 1); similar vertical distributions were also found in 1998 (Townsend *et al.*, 2001). Discrete bottle samples do not provide continuous concentration distributions, but there are many examples of subsurface and bimodal concentration maxima corresponding with the nitracline (Table I). The prevalence of subsurface and bimodal concentration maxima varies depending on conditions. During three cruises in the Gulf of Maine, bimodal concentration distributions were found between 10% and 40% of the time, more frequently when the nitracline was relatively deep ($>$20 m).

A diel cycle of positive phototaxis during the day and positive geotaxis at night has been proposed as the migratory strategy for *A. tamarense* in nutrient-limited environments (MacIntyre *et al.*, 1997; Fauchot *et al.*, 2005a). When surface waters are replete with nitrogen, *A. tamarense* in a shallow salt pond was shown to optimize its vertical position for irradiance and still fulfill its nutrient demands (Anderson and Stolzenbach, 1985). If the nitracline is deeper than the light penetration for optimal growth, then vertical migration can enhance overall production. After migrating to the nitracline, *A. catenella* can assimilate and store nutrients, altering cellular nitrogen by a factor of 5 depending on conditions (Collos *et al.*, 2004). Laboratory experiments have shown that *A. tamarense* cells collect near a light source in nitrogen-replete solution, but in nitrogen-deficient conditions, the organisms can migrate nocturnally toward nutrients (Rasmussen and Richardson, 1989; MacIntyre *et al.*, 1997). However, observations of *A. tamarense* (Anderson and Stolzenbach, 1985; MacIntyre *et al.*, 1997) as well as other dinoflagellate species (Eppley *et al.*, 1968; Cullen and Horrigan, 1981; Heaney and Eppley, 1981) indicate that the migration cues are not necessarily only light and dark, as organisms may begin descending before sunset or begin ascending before sunrise. Other observations indicate even more complex phasing between vertical distribution of dinoflagellates and the diel irradiance cycle (Passow, 1991; Kamykowski, 1995; Fauchot *et al.*, 2005a). Generalizations are difficult because different isolates of the same species can exhibit vastly different migration strategies, or no migration at all (J. Cullen, Halifax, personal communication).

One problem with laboratory studies of vertical migration is that experimental conditions do not necessarily scale well to oceanic observations. Vertical swimming speeds for *A. fundyense* and similarly sized dinoflagellates (diameter $\sim$40 μm) are typically between 5 and 15 m day^{-1} (Anderson and Stolzenbach, 1985; Bauerfeind *et al.*, 1986; Kamykowski & McCollum, 1986; Kamykowski *et al.*, 1992), and can be as high as 24 m day^{-1} (Eppley *et al.*, 1968). At these rates, organisms can traverse a laboratory column of a few meters length in roughly an hour, and therefore can synchronize their migration cycle with the photoperiod. However, subsurface concentrations of *A. tamarense* and *A. fundyense* cells have been found near nitraclines that are 25–40 m deep and below the mixed layer (Holligan *et al.*, 1984; Townsend *et al.*, 2001, 2005a), in which case migration for nutrient retrieval would require several days of swimming for a complete cycle. On the basis of simple scaling, diel migration synchronized to the photoperiod is not possible between organism populations at the surface and at a nitracline several 10s of meters below the surface.

Observations of *A. tamarense* in the St Lawrence estuary provide some indication of asynchronous

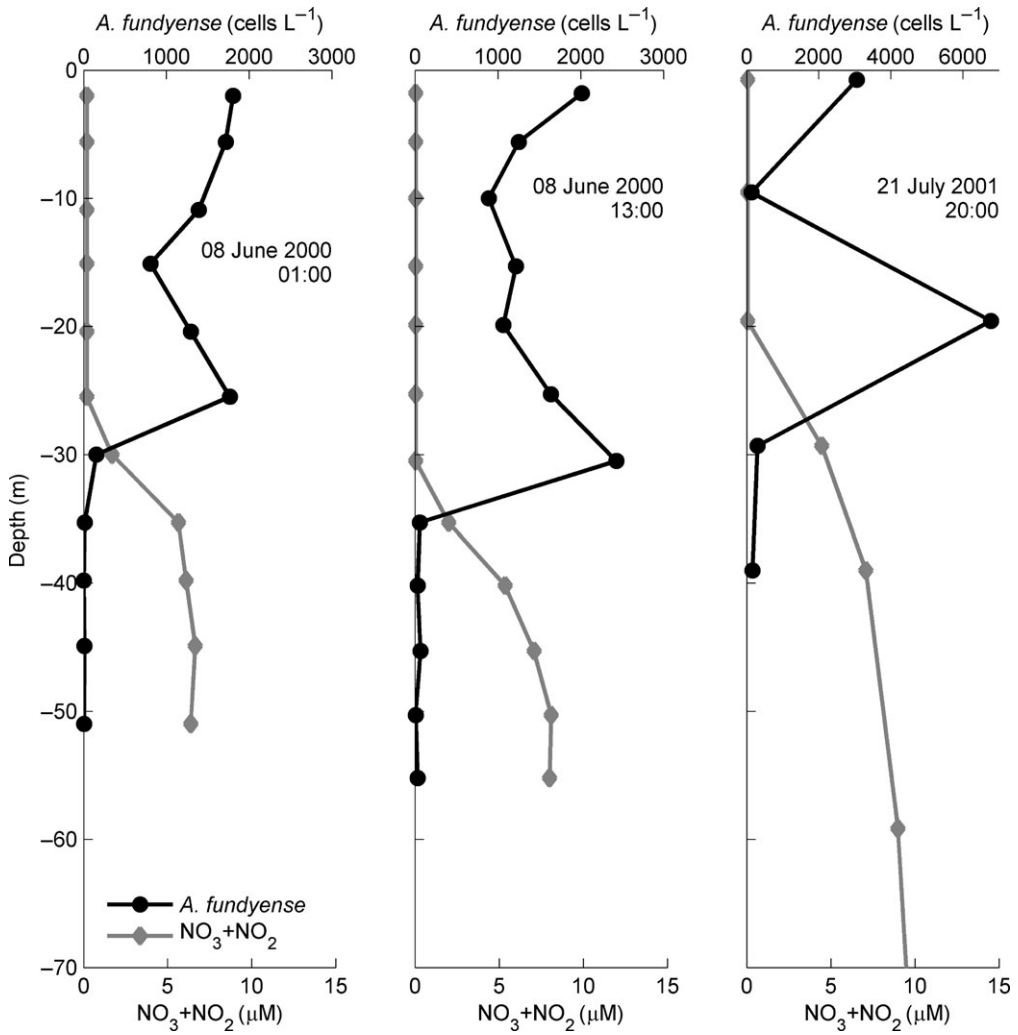

Fig. 1. Selected observations from the Gulf of Maine during June 2000 and July 2001, with *A. fundyense* cell concentration and combined nitrate and nitrite concentration.

Table I: Summary of A. fundyense vertical concentration profiles from three cruises in the Gulf of Maine

		Surface maximum (no. casts)		Subsurface maximum (no. casts)		Bimodal distribution (no. casts)		Fraction bimodal	
Cruise (total no. casts)	Nutrient conditions	>50	>1000	>50	>1000	>50	>1000	>50 (All cell conc.)	>1000 cells L^{-1} (High cell conc.)
June 2000 (141)	All N conditions	40	6	32	5	28	8	0.28	0.42
	Nitracline>20 m	19	6	18	5	25	7	0.40	0.39
July 2001 (142)	All N conditions	31	15	53	31	17	7	0.17	0.13
	Nitracline>20 m	5	0	28	18	13	7	0.28	0.28
July 2005 (27)	All N conditions	12	4	7	4	2	0	0.10	0.00
	Nitracline>20 m	1	0	4	2	1	0	0.17	0.00

Casts with cell concentrations >50 cells L^{-1} are categorized as having surface concentration maxima, subsurface maxima or bimodal concentration distributions. Columns distinguish moderate (>50 cells L^{-1}) and high (>1000 cells L^{-1}) concentrations, and rows distinguish nutrient conditions when the nitracline was 20 m or more below the surface.

vertical migration for nutrient retrieval (Fauchot *et al.*, 2005a). During a 48-h study period, high concentrations of organisms were found near the surface and near the nitracline. The authors proposed that the organisms retrieve nutrients at night and return to the surface during the day, thus implying a vertical swimming speed of 43–48 m day^{-1} when the nitracline was 12 m below the surface. The vertical migration was not strictly coordinated, as during one of the nocturnal sampling periods, concentrations of cells were found simultaneously near the surface and near the nitracline. The swimming velocity was calculated based on displacement of the concentration maximum, but it is quite large compared with other measurements of swimming velocities for dinoflagellates (Heaney and Eppley, 1981; Bauerfeind *et al.*, 1986; Kamykowski and McCollum, 1986; Kamykowski *et al.*, 1992), and *A. tamarense* in particular (Anderson and Stolzenbach, 1985). In a laboratory study of the effects of temperature on dinoflagellate swimming speeds, most of the 11 species tested displayed swimming speeds between 9 and 17 m day^{-1} when water temperature was between 10°C and 15°C (Kamykowski and McCollum, 1986). Water temperatures during the St Lawrence study were between 10°C and 13°C (Fauchot *et al.*, 2005a), and during the Gulf of Maine studies, water temperatures were 7°C to 12°C (Townsend *et al.*, 2001).

To reconcile the discrepancy between swimming speed and nitracline depth, we propose an alternative hypothesis that the *A. fundyense* vertical migration cycle is not confined to a diel period. Other phytoplankton species reportedly migrate between the surface and the nitracline over a period greater than 1 day (Cullen and MacIntyre, 1998). Rather than synchronous diel migration of positive phototaxis during the day and positive geotaxis with nutrient uptake at night, individual organisms may direct their migration based on their internal nutritional state (Cullen, 1985; Kamykowski, 1995; Kamykowski and Yamazaki, 1997; MacIntyre *et al.*, 1997; Flynn and Fasham, 2002). Regardless of the photoperiod, organisms that are nitrogen deficient tend to swim down toward the nitracline, and organisms that are nitrogen replete swim up toward the surface. Taken as a population average, this behavior can produce a range of vertical distribution patterns depending on nitracline depth and swimming speed, from uniform cell concentration to concentration maxima at the surface, at the nitracline or both.

In this work, we test the hypothesis that the bimodal distributions of *A. fundyense* that have been observed in the field can be the result of vertical migration for nutrient retrieval over periods longer than the diel photoperiod. We recognize that other explanations are possible, such as separate subpopulations with different physiological characteristics residing in the separate peaks. In this study, we investigate whether the observed bimodal distributions can be created by a single population with identical photosynthetic, nutrient uptake and migration capabilities. We apply a water column numerical model using the Lagrangian Ensemble method to track particles representing groups of organisms. We compare the model results with observations, and develop analytical tools to predict vertical distributions of cell populations based on conditions in the water column and growth and nutrient uptake characteristics of the organism.

METHOD

Model formulation

To represent independent trajectories for a large number of organisms, we develop an individual-based, one-dimensional numerical model using the Lagrangian Ensemble method (Woods and Barkmann, 1994; McGillicuddy, 1995; Broekhuizen, 1999). The Lagrangian Ensemble approach explicitly tracks a number of individual particles that move through the water column. Each particle represents a set of physiologically identical organisms that grow, move and die together based on ambient conditions. Water column properties are defined on an Eulerian grid and include irradiance, temperature, nutrient concentrations and turbulence intensity. Grouping phytoplankton into clusters (simulated as "particles") rather than following the trajectories of individual organisms makes the problem computationally manageable, yet retains important advantages of the Lagrangian framework. Specifically, the net population depends on integrated life histories of the individual particles, as opposed to a concentration-based Eulerian approach that cannot incorporate memory of previous environmental or physiological conditions for organisms with different trajectories.

The model developed for this study is largely based on previously published work (Broekhuizen, 1999; Broekhuizen *et al.*, 2003), but we have modified the model framework and input parameters to better represent vertical migration of *A. fundyense* in the Gulf of Maine. Each particle in the model has attributes of average cell mass (mg C) and nutrient content (mg N), and the physiological state of the cell depends on the ratio of these values (N:C). Cellular carbon increases with photosynthesis, which depends on the ambient light; cellular nitrogen increases through nutrient uptake, which depends on the ambient concentration of

nitrogen as well as the uptake parameters for the organism. The organisms are motile, so particles adjust vertical position depending on their nutrient needs. Organisms swim toward the surface when their internal N:C is high, grow rapidly in the surface layer where nutrient concentrations are low, and thereby decrease N:C. Organisms then swim downward toward the nitracline to resupply with nutrients, ceasing downward migration upon reaching high nutrient concentrations. In addition to active migration, particles change position because of turbulent mixing. Turbulence is parameterized with a turbulent mixing coefficient and accounts for spatial non-uniformity in turbulent diffusivity (Visser, 1997; Ross and Sharples, 2004).

Within each particle, the number of organisms varies depending on growth conditions. When average cell mass in a particle grows to a threshold mass for fission, cells divide and the cell mass becomes half the previous value, but the number of organisms in the particle doubles. Similarly, when cell size decreases below a threshold mass for starvation, that particle is removed from the model. In addition to the discrete fission and removal events, a background mortality rate continuously decreases the number of organisms in all particles. Thus the number of organisms in each particle varies, although the total number of particles is maintained such that no particle become excessively large or small. A more detailed description of the model including governing equations can be found in the Appendix.

Model parameters

The model relies on input parameters that describe response of the organisms to environmental conditions. Parameters used for the base simulation are listed in Table II, along with the ranges of parameters tested for model sensitivity. Biological input parameters such as growth rate, basal metabolism, nutrient uptake rate, cell size and cellular nitrogen content were determined for *A. fundyense* based on published values from laboratory, field and other modeling studies. Because estimates for all parameters were not available for *A. fundyense* or *A. tamarense*, we also drew data from studies of *A. catenella* and *A. taylori*. To initialize the model, particles are randomly distributed through the water column, and particle size and nutritional state are randomized within the physiological limits.

The physical grid of nutrient and light profiles parametrically reproduces a water column in the Gulf of Maine during late spring or early summer (Townsend *et al.*, 2001, 2005a). For simplicity, we assume that all of the DIN is in the form of nitrate, and refer to this nutrient concentration simply as nitrogen. The model could be adapted to include other sources of inorganic nitrogen such as ammonium or nitrite with appropriate adjustments to the uptake kinetics and vertical distributions. The nitracline is set 25 m below the surface, with low nitrogen concentration above the nitracline (0.05 μM) and higher concentrations below (5 μM) (Fig. 2). The concentration below the nitracline is large compared with the half-saturation constant for uptake of nitrogen ($k_N = 1$ μM), so higher concentrations would not enhance nitrogen uptake rates. The nitrogen concentration profile remains constant, based on an assumption that *A. fundyense* composes a small portion of the total phytoplankton community, and therefore does not significantly alter ambient nutrient concentrations.

The turbulent mixing parameterization is intended to represent a surface mixed layer of moderate turbulence intensity. The turbulent diffusivity profile is modeled after observations on the New England shelf during May and June 1997 (MacKinnon and Gregg, 2005). Turbulent diffusivity (K_z) decreases with depth from the surface, and depends on surface wind stress and water column stratification. With moderate wind speed ($U_{10} = 4\ \mathrm{m\ s^{-1}}$) and moderate stratification ($\mathcal{N}^2 = 5 \times 10^{-5}\ \mathrm{s^{-2}}$), the turbulent diffusivities are $K_z = 1 \times 10^{-3}\ \mathrm{m^2\ s^{-1}}$ at the surface and $8 \times 10^{-5}\ \mathrm{m^2\ s^{-1}}$ at the nitracline. This corresponds with K_z found from microstructure data on the New England Shelf (MacKinnon and Gregg, 2005), but is somewhat greater than estimates of K_z based on dye studies in the thermocline in Massachusetts Bay during the summer ($K_z \sim 6 \times 10^{-6}\ \mathrm{m^2\ s^{-1}}$) (Geyer and Ledwell, 1994). The turbulent diffusivities in the base simulation are within the range of K_z observed in the upper ocean, which can vary over three orders of magnitude or more (Denman and Gargett, 1983).

Alternative model formulations are possible, but we have chosen this framework to specifically investigate how relative time scales of growth, nutrient uptake and vertical migration impact the vertical distribution of organisms. In particular, we are interested in whether or not the bimodal vertical distributions of *A. fundyense* observed in the field may be symptomatic of asynchronous vertical migration. Other modeling studies of *A. fundyense* have incorporated additional complexity: multiple nutrients (nitrate, ammonium and phosphate), evolution of ambient nutrient concentrations, photoacclimation, biomass-dependent light attenuation and toxin production (Flynn, 2002; Flynn and Fasham, 2002; John and Flynn, 2002). Because we assume here that *A. fundyense* represents a relatively small fraction of the total phytoplankton community, these organisms have minimal impact on the ambient nutrient concentration and light attenuation. Similarly, the nutrient and

Table II: Model input parameters, range of parameters tested for sensitivity, and references

Variable	Description	Units	Initial conditions		
P_A	Cells per particle	cells ens^{-1}	P_{A0} = 1000+{0,500}		
P_C	Cellular carbon	mg C cell^{-1}	P_{C0} = {$W_{fission}$, W_{starve}}		
P_N	Cellular nitrogen	mg N cell^{-1}	P_{N0} = {NC_{min}, NC_{max}} P_{C0}		
z_p	Particle elevation	m	z_{P0} = {0,z_N}		
Parameter	**Description**	**Units**	**Base**	**Range**	**Reference**
Cell growth					
U_{MC}	Max growth rate	day^{-1}	0.65	0.35–0.95	Flynn *et al.*, 1996; MacIntyre *et al.*, 1997; Smayda, 1997; Yamamoto *et al.*, 2002; Fauchot *et al.*, 2005b; Garcés *et al.*, 2005; Stock *et al.*, 2005
α	Initial slope PI curve	day^{-1} (μmol photons m^{-2} s^{-1})	0.08	0.05–0.15	Stock *et al.*, 2005
m_{0C}	Basal metabolism rate	day^{-1}	0.10	0.05–0.15	McGillicuddy *et al.*, 2005; Stock *et al.*, 2005
Nitrogen uptake					
U_{MN}	Max N uptake rate	mg N mg^{-1} C day^{-1}	0.20	0.05–0.40	MacIsaac *et al.*, 1979; Tett and Droop, 1988; Collos *et al.*, 2004
k_N	Half saturation for N	μM	1	0.3–3.0	MacIsaac *et al.*, 1979; Tett and Droop, 1988; Smayda, 1997; Collos *et al.*, 2004; Collos *et al.*, 2005; Stock *et al.*, 2005
e_{Nmax}	Max N excretion rate	mg N mg^{-1} C day^{-1}	0.05		Assumed
Vertical migration					
w_{swim}	Swimming rate	m day^{-1}	10	4–16	Anderson and Stolzenbach, 1985; Bauerfeind *et al.*, 1986; Heaney and Eppley, 1986; Kamykowski *et al.*, 1992
w_{sink}	Sinking rate	m day^{-1}	0		Assumed
C_{down}	Trigger to swim down		0.15		Assumed
C_{up}	Trigger to swim up		0.85		Assumed
Cell physiology					
NC_{max}	Max N:C ratio		0.23	0.14–0.26	Tett and Droop, 1988; Anderson *et al.*, 1990; Flynn *et al.*, 1996; MacIntyre *et al.*, 1997; Collos *et al.*, 2004
NC_{min}	Min N:C ratio		0.06		
$W_{fission}$	Mass for cell division	mg C	2.3×10^{-6}		Anderson *et al.*, 1990; Flynn *et al.*, 1996; Collos *et al.*, 2004
W_{starve}	Mass for cell death	mg C	0.6×10^{-6}		
Δ_0	Background death rate	day^{-1}	0.10		Yamamoto *et al.*, 2002; Stock *et al.*, 2005
Grid					
z_N	Nitracline depth	m	25	10–80	Townsend *et al.*, 2001; Love *et al.*, 2005; Townsend *et al.*, 2005a
N_{min}	N above nitracline	μM	0.05		
N_{max}	N below nitracline	μM	5		
E_{0max}	Max surface irradiance	μmol photons m^{-2} s^{-1}	1200		McGillicuddy *et al.*, 2005
T_{day}	Length of daylight	h	16		Assumed
k_E	Background attenuation	m^{-1}	0.20		Townsend *et al.*, 2001; Townsend *et al.*, 2005a
U_{10}	Wind velocity	m s^{-1}	4	1–9	MacKinnon and Gregg, 2005
N^2	Buoyancy frequency	s^{-2}	5×10^{-5}		
K_z ($z = 0$)	Turbulent diffusivity, surface & nitracline	m^2 s^{-1}	1×10^{-3}	10^{-4}–10^{-2}	
K_z ($z = z_N$)			8×10^{-3}	10^{-5}–10^{-3}	

Initial conditions are randomized, with {a,b} indicating a random value between a and b.

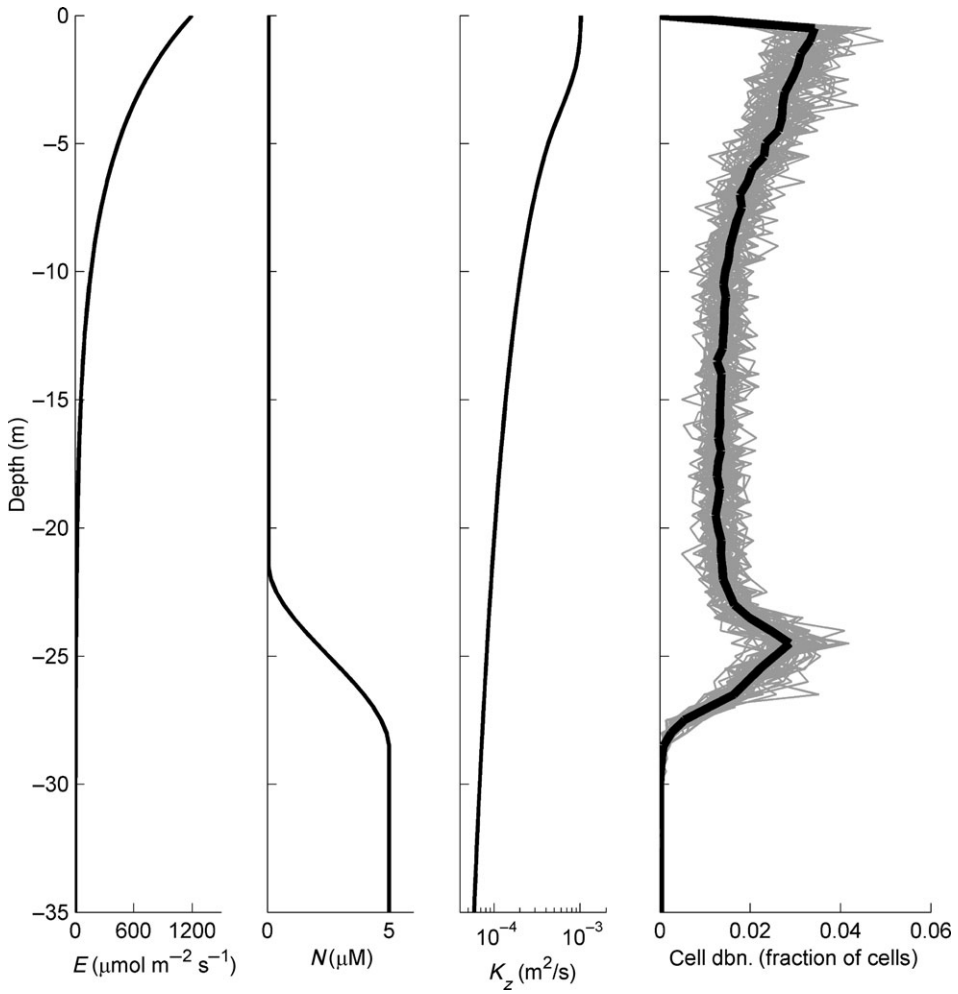

Fig. 2. Vertical profiles of irradiance, nitrogen concentration, turbulent diffusivity and relative cell distribution through the water column. Cell distribution is normalized by the total number of cells in the water column; the gray lines are individual profiles over a 9 day period and the black line is the average over the 9 days.

turbulence profiles have been based on field conditions so that model results can be compared with observations. On the basis of the mechanisms in this simplified framework, we can progressively expand the analysis to include additional physical and biological processes.

Data collection

Vertical profiles of nutrient concentrations and *A. fundyense* cells were measured in the coastal and offshore Gulf of Maine during research cruises from 5–14 June 2000, 19–28 July 2001 and 1–3 July 2005, aboard the *R/V Cape Hatteras*. Collection methods were those described by Townsend *et al.* (Townsend *et al.*, 2005a, b). Briefly, water samples along with CTD data were acquired using a SeaBird CTD and carousel water sampler equipped with 5 L Niskin bottles. For most stations, five standard depths were sampled, at the surface (1–2 m), 10, 20, 30 and either 40 or 50 m. Nutrient samples were filtered through Millipore HA filters, placed immediately in a sea water-ice bath for 5–10 min, and frozen at −18°C to be analyzed following the cruises for NO_3+NO_2, NH_4, $Si(OH)_4$ and PO_4 using an autoanalyzer and standard techniques. Enumerations of *A. fundyense* cell densities were made by sieving 2 L of water from each sample depth through a 20 μm mesh screen; the concentrate was preserved in a 5% formaldehyde sea water solution and stored in 20 ml vials in the dark in a refrigerator. Quantitative cell counts were performed within 14 months of collection, and were based on epifluorescence microscopy and an immunological stain specific to the genus *Alexandrium*; details are given in Townsend *et al.* (Townsend *et al.*, 2005a, b). During the June 2000 cruise, we sampled two stations at hourly intervals over

a period of 25 h, collecting water at 5-m depth intervals (Townsend *et al.*, 2005a).

RESULTS

Model results

The model base simulation produces a bimodal vertical distribution of *A. tamarense*, with maximum concentrations located near the surface and near the nitracline, based on instantaneous profiles or an average over a longer period (Fig. 2). The results shown are 40 days after the start of the simulation; the vertical distribution has reached steady state. The total number of organisms in the system grows exponentially in this simulation (doubling time growth rate $k \sim 0.15\ \text{day}^{-1}$), but we are primarily interested in the relative positioning of organisms in the water column rather than absolute concentrations. The population growth rate depends on the background mortality rate, and that is poorly constrained because it integrates many processes not explicitly addressed in the model (e.g. grazing pressure, natural attrition, encystment). To account for variability in absolute growth rate between simulations, vertical cell distributions are normalized by the total number of cells in the water column.

The vertical distribution of the population depends on the sum of the independent trajectories of the particles. The vertical migration cycle is shown graphically for three representative particles in Fig. 3. The variable controlling vertical positioning is the nutrient

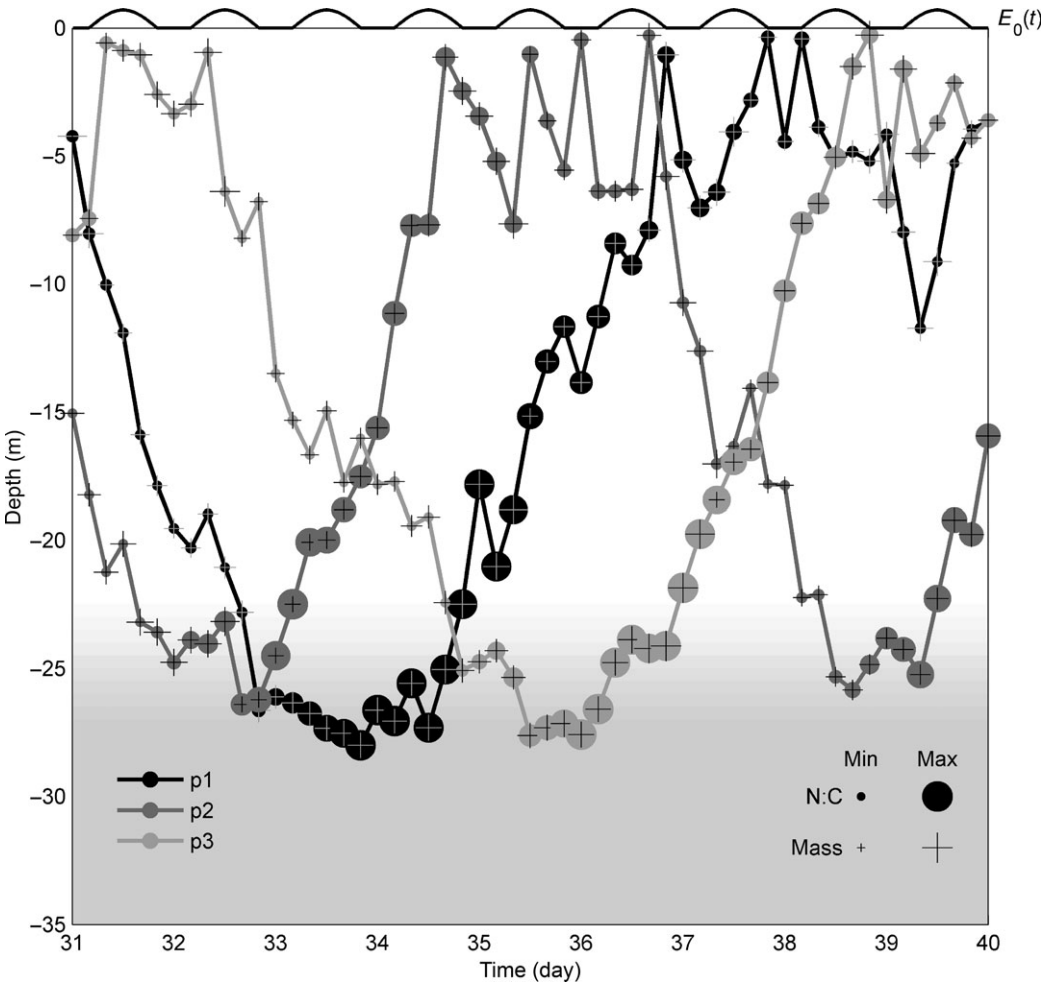

Fig. 3. Trajectories of three particles (labeled p1, p2 and p3), depicting N:C ratio (circle size, scaled between $N:C_{min}$ and $N:C_{max}$) and cell mass (cross size, scaled between W_{starve} and $W_{fission}$). Background shading indicates water column nitrogen concentration, from 0.05 μM at the surface to 5 μM at the bottom. Diel variation in irradiance is shown schematically at the top of the plot. N:C increases near the nitracline when nutrient uptake is faster and growth is slower, and decreases away from the nitracline where nitrogen uptake is slower and cell growth faster. Cell mass increases because of photosynthesis, and decreases due to cell division or respiration during periods of darkness or low light.

ratio N:C. In *A. fundyense* and in other dinoflagellates, the nutrient ratio can vary over a wide range, decreasing when nutrients become scarce and increasing when nutrients are plentiful (Cullen and Horrigan, 1991; Anderson *et al.*, 1990). As the organisms accumulate nitrogen at depth, N:C increases up to the physiological limit for nutrient storage; for *A. fundyense*, $N:C_{max}$ is $\sim$0.23 on a mass basis (Anderson *et al.*, 1990; Flynn *et al.*, 1996; MacIntyre *et al.*, 1997; Collos *et al.*, 2004). The rate of nitrogen uptake is implicitly linked to the ambient light by virtue of its dependence on phytoplankton carbon content (Appendix). Consequently, nitrogen uptake slows to the extent that cellular energy reserves diminish, as respiratory demands are not fully met by carbon fixation in the dimly lit waters of the nutricline. To first order, the modeled uptake kinetics mimic the observations that uptake of nitrogen (particularly nitrate) can be significantly reduced in low light conditions (MacIsaac, 1978; Cochlan *et al.*, 1991; Kudela *et al.*, 1997; Flynn and Fasham, 2002).

Once cells in the nitracline have reached capacity for nutrient uptake, the organisms migrate upward toward the surface. The transit up takes 2–3 days [$t \sim z_N / w_{swim} \sim (25\text{ m})/(10\text{ m day}^{-1})$], and as they swim upward the organisms increase photosynthesis, generally increasing cellular carbon and decreasing N:C. Photosynthesis is rapid near the surface because of high light levels, but at the nitracline respiration exceeds light-limited photosynthesis, and cell mass decreases. Decreases in cell mass are also due to discrete division events when cells grow to their maximum size and divide, and due to respiration during hours of darkness or low irradiance. If the cells reach the surface and N:C remains greater than the physiological minimum [$N:C_{min} \sim 0.06$ on a mass basis (Anderson *et al.*, 1990; MacIntyre *et al.*, 1997; Collos *et al.*, 2004)], they remain at the surface and continue to add carbon, but nitrogen uptake is negligible because of the low ambient concentration. Finally, once N:C has decreased to minimally tolerable levels, the organisms swim back down toward higher nutrient concentrations. In the base simulation, one complete migration cycle takes 8–9 days.

The migration cycle can also be described by considering organism N:C ratio as a function of vertical position in the water column (Fig. 4). At the nitracline, organisms hold position as they accumulate nitrogen and increase N:C. When they are full of nutrients, they swim toward the surface, photosynthesizing during the transit and decreasing N:C. In this base simulation, they continue to grow when they reach the surface until they approach $N:C_{min}$. The organisms then swim downward to retrieve nutrients, completing the cycle.

Sensitivity testing

Vertical distributions of cells in the model are sensitive to properties of the organisms and of the water column. The characteristics that most directly impact vertical distribution are the cell growth rate, the nitrogen uptake rate, the vertical excursion rate (swimming speed and turbulence) and the intensity of vertical mixing. Each of the three migratory phases depends on several factors—growth depends on the maximum photosynthetic rate (U_{MC}), the growth efficiency (α) and the irradiance profile; nitrogen uptake depends on the maximum uptake rate (U_{MN}), the half-saturation constant (k_N) and the nitrogen concentration profile; and migration time depends on the swimming speed (w_{swim}) and the distance between the surface and the nitracline (z_N). To test the sensitivity of the model, each of these parameters can be varied independently over a range of plausible values. We describe examples of the impact of changing input parameters on the relative duration of the three phases, but note that similar results emerge from changes to related parameters. For example, increasing the maximum photosynthetic rate has a similar effect as increasing the surface irradiance, and decreasing the swimming velocity is similar to increasing the distance between the surface and the nitracline. We also consider how changes in turbulent mixing alter the homogeneity of the vertical concentration profiles.

Altering the maximum growth rate changes the amount of time organisms spend near the surface (Fig. 5a). When U_{MC} increases, organisms grow faster both at the surface and during the transit up through the water column, so as a result they spend less time in the near-surface layer before returning to the nitracline. When U_{MC} decreases, photosynthesis is slower, so more time is spent at the surface relative to near the nitracline. Changes to the maximum nitrogen uptake rate have the opposite effect (Fig. 5b). Increasing U_{MN} decreases the amount of time required to absorb a body load of nitrogen, so relatively more time is spent near the surface. Decreases to U_{MN} mean slower nutrient uptake, so organisms spend longer at the nitracline during each cycle. Note that the concentration profiles are normalized to total cell mass because changes to the photosynthesis and uptake parameters significantly alter the net growth rate.

Altering swimming speed changes the amount of time organisms spend migrating between the nitracline and the surface, but it can also change the time organisms spend at the surface (Fig. 5c). For faster swimming speeds, transit time and organism concentration midwater column are both lower; for slower swimming speeds, more of the migration cycle is spent between

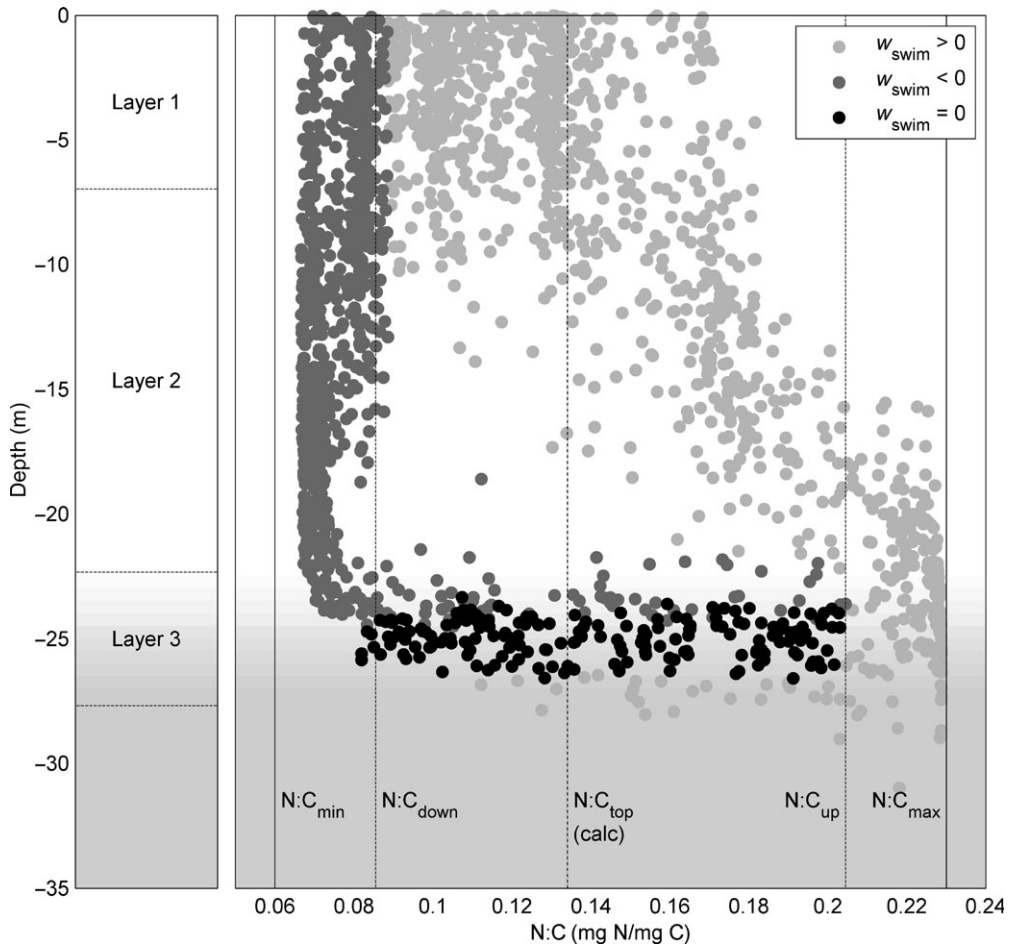

Fig. 4. Instantaneous N:C ratio for all particles as a function of particle depth, noting swimming direction with color. The locations of the surface (layer 1), mid-water column (layer 2) and nitracline (layer 3) layers are also shown to the left, and the background shading indicates water column nitrogen concentration. Vertical lines show values for maximum and minimum N:C (N:C_{max} and N:C_{min}), values of N:C at which organisms begin vertical migration (N:C_{down} and N:C_{up}), and the analytical estimate for N:C when organisms reach the surface (N:C_{top}).

the surface and the nitracline. Because organisms photosynthesize as they swim upward, the time spent mid-water column impacts the nutrient ratio N:C when they arrive at the surface. With slow swimming speeds, N:C may decrease during the upward migration to the lower physiological limit before the organisms reach the surface. If so, the organisms turn around and swim back downward to retrieve nutrients, and the net effect is to decrease or eliminate the surface cell concentration maximum. This scenario creates high cell concentrations near the nitracline and more dispersed populations in the surface layer. Alternatively, if the nitracline is shallow enough that the irradiance is sufficient for rapid growth, then a single cell concentration maximum can form as the organisms cease vertical migration.

Finally, the model results depend on the amount of turbulent mixing in the water column (Fig. 5d). Turbulence adds a quasi-random component to the organism trajectories, so the primary effect of increasing K_z (or correspondingly, increasing the surface wind speed) is to broaden the surface and nitracline concentration maxima. The vertical distribution of organisms is more uniform, but the relative proportion of organisms in the surface and nitracline layers remains similar. Similarly, decreasing turbulent mixing allows the organisms to position themselves steadily near the surface or the nitracline. Effects of turbulence on mixing nutrients vertically are not included in the model, and would be important if mixing increased the vertical flux of nitrogen into the surface layer.

Analytical estimates

The vertical distribution of the *A. fundyense* population is proportional to the amount of time organisms spend in

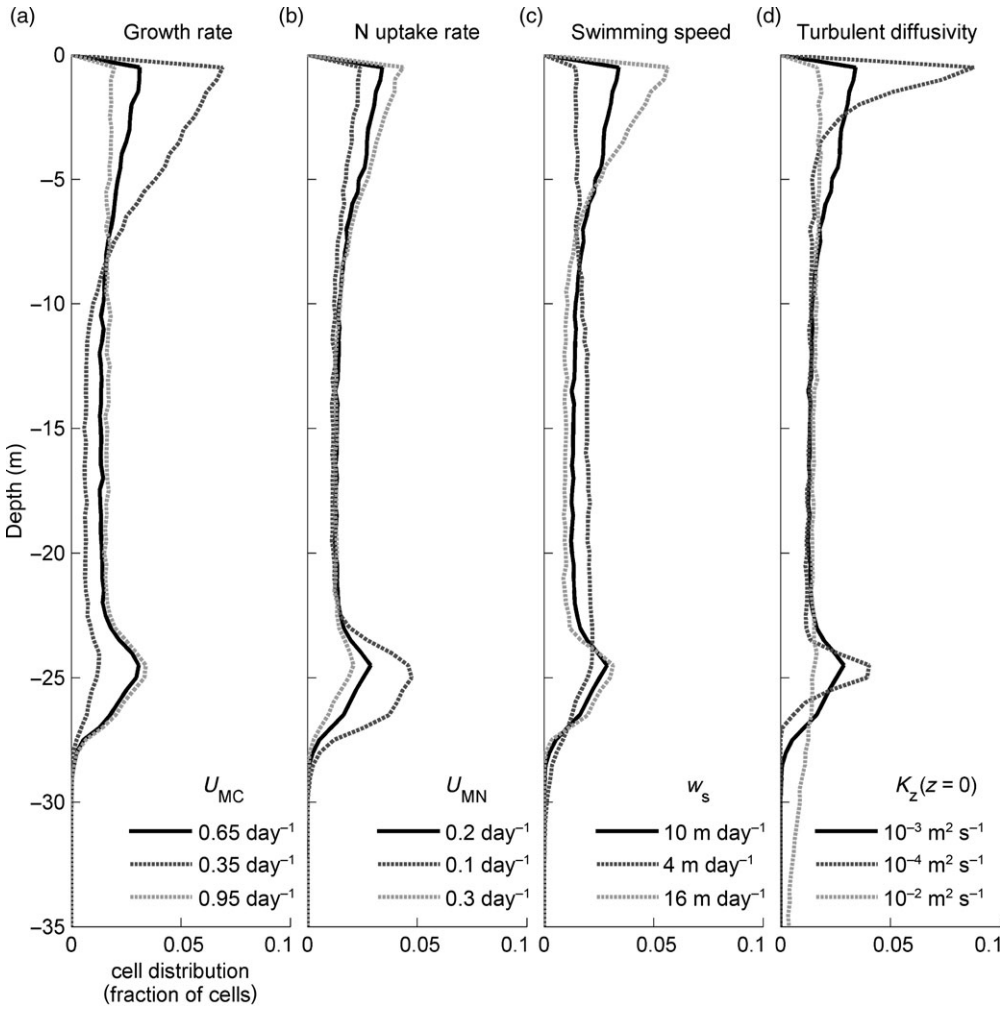

Fig. 5. Variations in relative cell distributions with changes in model input parameters: growth rate (U_{MC}), nitrogen uptake rate (U_{NC}), swimming speed (w_{swim}) and turbulent diffusivity (K_z). In all panels, the base simulation is plotted as a solid black line, and cases with higher and lower values are dashed lines. Cell distributions are normalized by the total number of cells in the water column, but the total number of cells varies with input parameters. For the turbulent diffusivity cases, the stated K_z are values at the surface, and K_z decreases with depth according to the formula in the Appendix. Surface K_z of 10^{-4} m^2 s^{-1} corresponds with a wind speed (U_{10}) of 2 m s^{-1}, and surface K_z of 10^{-2} m^2 s^{-1} corresponds with 9 m s^{-1} wind.

each part of the water column. With simplifying assumptions about uptake and growth rates in each layer, we can estimate what fraction of each migration cycle organisms spend in layers (1) near the surface, (2) in transit between the surface and nitracline and (3) near the nitracline, and calculate the relative distribution of organisms among the three layers (Fig. 4). The thicknesses of the surface and nitracline layers are defined based on length scales for turbulent diffusivity at each depth: $L \sim \sqrt{K_z \Delta t}$, where Δt is the average time organisms spend in each layer. Organism concentration in each layer is equal to the time spent there divided by the thickness of the layer: $C_1 \sim t_1/h_1$, $C_2 \sim t_2/h_2$ and $C_3 \sim t_3/h_3$. In the upper layer, the time scale is based on the growth rate: $t_1 \sim 1/U_{MC}$; in the middle layer, the time scale is based on the swimming speed and the layer thickness: $(2h_2)/w_{swim}$; and in the lower layer, the time scale depends on the uptake rate and the cellular nitrogen ratio: $(N:C)/U_{MN}$.

On the basis of the input parameters for the base simulation ($U_{MC} = 0.65$ day^{-1}, $U_{MN} = 0.20$ day^{-1}, $w_{swim} = 10$ m day^{-1}, N:C$\sim$0.2), and assuming layer thicknesses of $h_1 = h_3 = 2.5$ m and $h_2 = 20$ m, the total cycle time is $\sim$7 days. The resulting concentration in the surface is $\sim$50% greater than the concentration in the bottom layer, and the bottom layer concentration is $\sim$100% greater than in the middle layer ($C_1:C_2:C_3 \sim 3:1:2$). This scaling approximates a bimodal concentration distribution, but we can improve the estimate with a more detailed analytical approach to the model equations.

The nutrient ratio N:C is the controlling variable in the model (NC in the following notation), so we solve for how the nutrient ratio varies with time:

$$\frac{\partial \mathrm{NC}}{\partial t} = \frac{\partial}{\partial t}\left(\frac{P_\mathrm{N}}{P_\mathrm{C}}\right) = \frac{(\partial P_\mathrm{N}/\partial t)P_\mathrm{C} - (\partial P_\mathrm{C}/\partial t)P_\mathrm{N}}{P_\mathrm{C}^2}, \quad (1)$$

where the P_N and P_C are cellular nitrogen and carbon, and the rates of change are the uptake rates:

$$\frac{\partial P_\mathrm{C}}{\partial t} = U_\mathrm{MC}\tanh\left(\frac{\alpha E_\mathrm{P}}{U_\mathrm{MC}}\right)P_\mathrm{C} - m_{0\mathrm{C}}P_\mathrm{C} = (U_\mathrm{C})P_\mathrm{C} \quad \text{and}$$

$$\frac{\partial P_\mathrm{N}}{\partial t} \approx \left[\frac{(U_\mathrm{mN})\mathcal{N}_\mathrm{p}}{(k_\mathrm{N}+\mathcal{N}_\mathrm{p})}\right]P_\mathrm{C} = (U_\mathrm{N})P_\mathrm{C}. \quad (2)$$

In the uptake formulas, U_MC is the maximum growth rate, α the growth efficiency, E_p the irradiance at the particle elevation, $m_{0\mathrm{C}}$ the respiration rate, U_MN the maximum nitrogen uptake rate, k_N the half-saturation constant and $\mathcal{N}_\mathrm{p}$ the nitrogen concentration at the particle (see Appendix for details); we have assumed that nitrogen excretion is negligible. If we rearrange equation (1) so that NC depends on the effective growth (U_C) and nutrient uptake rates (U_N),

$$\frac{\partial \mathrm{NC}}{\partial t} = U_\mathrm{N} - U_\mathrm{C}\mathrm{NC}, \quad (3)$$

then the solution for NC as a function of time is

$$\mathrm{NC}(t) = \frac{U_\mathrm{N}}{U_\mathrm{C}} + B\exp(-U_\mathrm{C}t), \quad (4)$$

where the coefficient B depends on initial conditions. A simplifying assumption for this solution is that uptake (U_N) and growth (U_C) rates do not vary in time. In the model, the uptake rates vary spatially with nitrogen concentration and irradiance, so we apply the solution piecewise to periods during which organisms experience relatively constant uptake rates. Note that the growth rate includes respiration and can be negative, but in these cases, photosynthesis exceeds respiration and net growth is greater than zero.

Starting when the organisms arrive at the nitracline, $\mathrm{NC}\sim\mathrm{NC}_\mathrm{min}$, so $B = \mathrm{NC}_\mathrm{min} - U_\mathrm{N}/U_\mathrm{C}$. Organisms remain near the nitracline until $\mathrm{NC} = \mathrm{NC}_\mathrm{up}$, so we solve for the time spent near the nitracline:

$$t_3 = -\ln\left(\frac{\mathrm{NC}_\mathrm{up} - (U_\mathrm{N}/U_\mathrm{C})_3}{\mathrm{NC}_\mathrm{min} - (U_\mathrm{N}/U_\mathrm{C})_3}\right)U_{\mathrm{C}3}^{-1}, \quad (5)$$

where the "3" subscripts indicate average growth and nitrogen uptake rates in layer 3. The time for transit between the nitracline and the surface is straightforward, $t\sim h_2/w_\mathrm{swim}$, where h_2 is the distance between surface and nitracline layers. Total time spent in the middle layer is twice this to account for swimming up and back down, so

$$t_2 = \frac{2h_2}{W_\mathrm{swim}}, \quad (6)$$

During the transit up, the organisms grow and NC decreases, so we solve for the nutrient ratio when the particles reach the surface. At the beginning of the ascent, $\mathrm{NC}\sim\mathrm{NC}_\mathrm{up}$, so $B = \mathrm{NC}_\mathrm{up} - U_\mathrm{N}/U_\mathrm{C}$. Using this constant and $t = z_\mathrm{N}/w_\mathrm{swim}$, the ratio at the surface is

$$\mathrm{NC}_\mathrm{top} = \mathrm{NC}_\mathrm{up} + \left(\frac{U_\mathrm{N}}{U_\mathrm{C}}\right)_2\left(1 - \exp\left(-U_{\mathrm{C}2}\frac{z_\mathrm{N}}{w_\mathrm{swim}}\right)\right). \quad (7)$$

Organisms remain at the surface as they grow from NC_top to $\mathrm{NC}_\mathrm{down}$. The initial condition when at the surface is $\mathrm{NC} = \mathrm{NC}_\mathrm{top}$, so $B = (\mathrm{NC}_\mathrm{top} - U_\mathrm{N}/U_\mathrm{C})\exp(-U_\mathrm{C}(z_\mathrm{N}/w_\mathrm{swim}))$. Solving for time spent at the surface,

$$t_1 = -\ln\left(\frac{\mathrm{NC}_\mathrm{down} - (U_\mathrm{N}/U_\mathrm{C})_1}{\mathrm{NC}_\mathrm{up} - (U_\mathrm{N}/U_\mathrm{C})_1}\right)U_{\mathrm{C}1}^{-1} - \frac{z_\mathrm{N}}{w_\mathrm{s}}. \quad (8)$$

Again, the concentration in each layer is proportional to the time spent there divided by the layer thickness. The ratio between the surface concentration (C_1) and the concentration near the nitracline (C_3) is an indication of the vertical distribution of the organisms: high C_1:C_3 for a surface population, low C_1:C_3 for a subsurface population, and C_1:$C_3\sim 1$ for a bimodal distribution (assuming $C_2 << C_{1,3}$, which is true for most of these simulations). The analytical estimates depend only on the input parameters for growth, uptake and migration, so we calculate C_1:C_3 over a range of parameter space. As in the model sensitivity testing, we note that photosynthesis and nitrogen uptake each depend on several variables, but we use the maximum growth and uptake rates to simulate effects of variability in the net rates. We convert the migration cycle phases into time scales to show how each impacts the vertical distribution: $t_\mathrm{growth}\sim 1/U_\mathrm{MC}$, $t_\mathrm{uptake}\sim(\mathrm{N{:}C})/U_\mathrm{MC}$ and $t_\mathrm{migration}\sim z_\mathrm{N}/w_\mathrm{swim}$.

The resulting maps of parameter space quantify trends implied by the sensitivity testing (Fig. 6). Slow

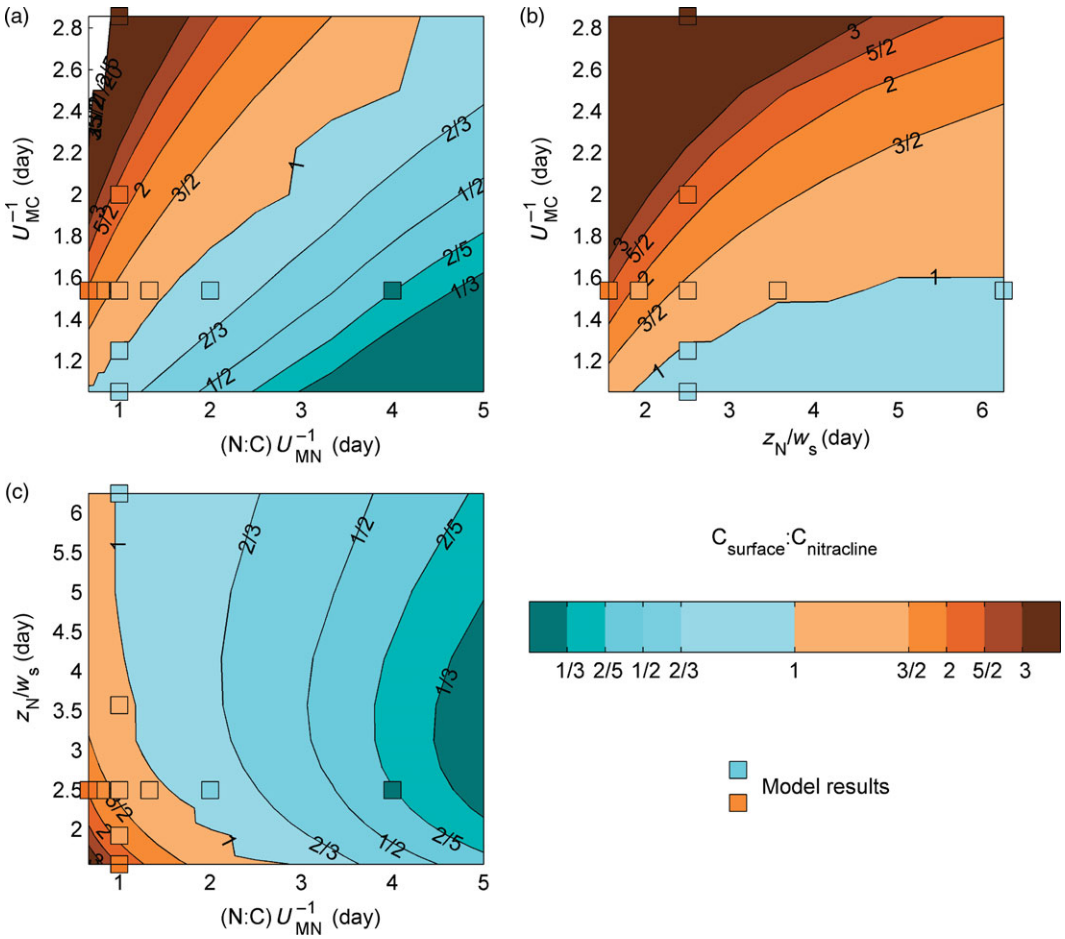

Fig. 6. Maps of ratios of cell concentration in the surface layer to cell concentration in the nitracline with variations in input parameters (converted into time scales: $1/U_{MC}$, $(N:C)/U_{NC}$, and z_N/w_{swim}). Color contours are based on the analytical calculation, and square markers show results from numerical model simulations.

growth (or large t_{growth}) produces surface concentration maxima (e.g. upper left corner of Fig. 6a), as organisms spend most of the time growing slowly at the surface and infrequently return to the nitracline. Slow nitrogen uptake (large t_{uptake}) creates subsurface maxima (e.g. lower right of Fig. 6a), as organisms take longer to accumulate a body load of nutrients. Similarly, slow migration (large $t_{migration}$) creates subsurface maxima (e.g. lower right of Fig. 6b) as organism grow significantly during the transit upward from the nitracline and must return for nutrients after a shorter (or no) time at the surface. Concentration distributions computed from model sensitivity runs are plotted along with the analytical parameter maps, and the agreement lends confidence to the scaling estimates. We can then use this approach to predict the vertical distribution of organisms based on characteristics of the organism (maximum growth rate, maximum uptake rate and half-saturation constant, swimming speed) and the environment (light profile and nutrient concentrations, depth of the nitracline).

DISCUSSION

The model results indicate that vertical migration for nutrient retrieval to a deep nitracline (~20–40 m) is plausible for *A. fundyense* even at moderate swimming speeds (~10 m day^{-1}). Important distinctions are that the migration cycle is not restricted to the diel photoperiod, but instead extends over several days, and that migration is not synchronous. The vertical distribution of *A. fundyense* cells depends on characteristics of the organisms (growth rate, nitrogen uptake rate, swimming speed) and the water column (nitracline depth, light penetration, turbulent mixing). Within reasonable ranges for these parameters, the model yields vertical profiles with surface, subsurface and bimodal cell

concentration maxima, all of which have been observed in the coastal ocean.

Vertical migration for nutrient retrieval is an advantageous survival strategy for dinoflagellates and other phytoplankton (Cullen, 1985), but by decoupling from strict diel phototaxis, *A. fundyense* may have the additional advantage of access to deeper pools of nutrients. Organism nutritional state may be the defining parameter for *A. fundyense* migration, as laboratory studies have shown that some *A. tamarense* strains remain at the surface when nitrogen is available throughout the water column, whereas other dinoflagellates continue with diel migration (MacIntyre *et al.*, 1997). Even with an extended migration period, the nitracline can be too deep for organisms to survive the transit between the nutrient uptake and the surface. For example, the population in the model with the base parameters steadily declines when the nitracline is greater than 60 m deep. Additionally, dinoflagellate swimming can be hindered by greater turbulence intensity when turbulent displacements greatly exceed swimming speeds or small-scale shear damages flagella (Smayda, 1997).

Although laboratory (MacIntyre *et al.*, 1997) and field observations (Fauchot *et al.*, 2005a) have inferred that *A. tamarense* can migrate with a diel period, a survey in the Gulf of Maine found no evidence for synchronous vertical migration (Townsend *et al.*, 2005a). Laboratory studies have shown that *A. tamarense* may not migrate vertically due to phototaxis when nutrients are plentiful throughout the water column (MacIntyre *et al.*, 1997) or absent from the entire water column (Rasmussen and Richardson, 1989), supporting the idea that nutrient retrieval is a dominant motivation for migration. Generally, laboratory studies have been limited by test columns with only 1 or 2 m between the nitracline and the light source. To directly address the balance between light and nutritional state in cueing vertical migration, longer experimental columns or slower swimming organisms would better maintain natural proportions among time scales for growth, nutrient uptake and migration.

Vertical migration of *Alexandrium* sp. based on the nutritional state can have consequences for the horizontal distribution of the organisms. In a shallow coastal pond without significant nutrient gradients, subsurface accumulation of *A. tamarense* reduced export associated with gravitational circulation at the mouth, and thereby increased organism residence time in the pond (Anderson and Stolzenbach, 1985). Similarly, sheared velocity profiles due to surface wind stress could differentially advect surface and subsurface populations, enhancing bloom dispersion. Velocity shear can be particularly strong in river plumes where stratification suppresses vertical mixing, and transport of *A. tamarense* in the Gulf of Maine has been linked to wind-driven advection of river plumes (Franks and Anderson, 1992; McGillicuddy *et al.*, 2003). Velocity shear can complicate field measurements of vertical migration. The rate of change of the vertical distribution of organisms can be linked to swimming speed only if lateral advection has not significantly altered the organism distribution at the sampling station (Passow, 1991; Townsend *et al.*, 2005a). Following a drifter to define a water mass for sampling may be ineffective when there is significant shear between the surface and the nitracline. Similarly, programs to map and provide warning of red tides due to *A. fundyense* should not be limited to surface samples, but should include measurements of vertical structure. Saxitoxin production in *A. fundyense* depends on organism nutritional state and ambient irradiance, and a Lagrangian model can incorporate these factors to simulate toxin concentrations and potential impacts (Flynn, 2002).

The numerical model used in this study included simplifying assumptions to narrowly focus on the question vertical migration of *A. fundyense* and *A. tamarense*. However, the Lagrangian Ensemble approach is potentially quite versatile, and the model could be modified to consider interactions between vertical migration and other important processes. For example, studies indicate that *A. tamarense* (Anderson and Stolzenbach, 1985; Fauchot *et al.*, 2005a) and other dinoflagellates (Ault, 2000) adjust their depth to optimize photosynthetic yield, so vertical migration rules could incorporate preferences for ambient irradiance in addition to nutritional state (Flynn and Fasham, 2002). Effects of photoadaptation (Woods and Barkmann, 1994; McGillicuddy, 1995) and turbulence (Barkmann and Woods, 1996; Kamykowski and Yamazaki, 1997) on motile organisms have been considered in Lagrangian models and could be incorporated to address accumulation of *A. catenella* in thin layers of low velocity shear and turbulence intensity (Sullivan *et al.*, 2003). For turbulent mixing, one could more realistically capture vertical and temporal variability by incorporating a water column turbulence model such as the General Ocean Turbulence Model (www.gotm.net). The Lagrangian approach could also be extended to more complex processes in the *A. fundyense* life cycle such as cyst formation, which requires interaction between organisms and is highly dependent on environmental conditions and nutritional state (Anderson *et al.*, 1984). Similarly, Lagrangian models could simulate interactions between water column nutrients and vertical migration by other mechanisms such as buoyancy regulation (Villareal *et al.*, 1993; Richardson *et al.*, 1998; White *et al.*, 2006).

Finally, the current model has been idealized with constant nutrient concentrations and light extinction to focus on vertical migration, and has excluded factors that could be important in field simulations. For example, organisms in the model do not alter the nutrient profile through consumption, but an alternative formulation might simulate a deepening nitracline as surface nutrients are depleted by the phytoplankton community. Along with consumption, nutrient profiles could also depend significantly on vertical turbulent fluxes with variable wind forcing, and in three-dimensional applications, nutrient profiles may depend on lateral advection and interleaving of different water masses. Although this model focused on a single nutrient, a more complete model could include ambient concentrations and organism uptake rates for multiple nitrogen species (nitrate, nitrite and ammonium) and for phosphate (Flynn and Fasham, 2002). Similarly, water column irradiance depends on spatially and temporally variable light attenuation, and high biomass concentrations that limit light penetration can provide a control on vertical migration (Flynn and Fasham, 2002). Because of the sensitivity of these biological models to rather poorly-constrained input parameters, any results should be interpreted in conjunction with robust laboratory and field observations.

ACKNOWLEDGEMENTS

The authors thank Maura Thomas for assistance processing field data, and Don Anderson for comments on a draft manuscript. The authors thank two anonymous reviewers and the editor for thoughtful comments.

FUNDING

Postdoctoral Scholar Program at the Woods Hole Oceanographic Institution by the J. Seward Johnson Fund to D.K.R.; CSCOR ECOHAB Program through NOAA grant (NA06NOS4780245); Woods Hole Center for Oceans and Human Health; National Science Foundation (Grant OCE-0430724); National Institute of Environmental Health Sciences (Grant 1-P50-ES012742-01) to D.J.M.

APPENDIX

This Lagrangian Ensemble model builds largely off work by Broekhuizen *et al.* (Broekhuizen, 1999; Broekhuizen *et al.*, 2003). For this application, some of the equations have been modified, and in many cases simplified; for example, we removed the temperature dependence of growth and uptake rates included in the original model. The input parameters are for dinoflagellates (Broekhuizen *et al.*, 2003), but have been adjusted based on a literature survey to be specific to *A. fundyense*.

At each time step, the model updates the composition and position of each Lagrangian particle. Composition includes cellular mass (P_C, mg C cell^{-1}) and nutrient content (P_N, mg N cell^{-1}), and the total number of organisms within the particle (P_A); water column cell concentrations then depend on the vertical distribution of particles and on the organism population within each particle. Particle positions depend on swimming speed (w_{swim}) and on displacements due to turbulent fluctuations. Eulerian profiles of nitrogen and turbulent diffusivity are held constant through the simulation, but incident irradiance is varied diurnally. The Eulerian grid discretization is 0.5 m to resolve water column structure, and the model time step is set so that Lagrangian particles do not cross through a grid cell in a single time step. The grid is sufficiently deep that particles do not encounter the bottom.

Cellular carbon (P_C, mg C cell^{-1})

Cellular carbon increases with photosynthesis and decreases with metabolism. Photosynthetic growth is formulated as in Jassby and Platt (Jassby and Platt, 1976), but an alternative formulation (Smith, 1936) yields very similar results.

$$\frac{dP_C}{dt} = \text{photosynthesis - metabolism} = u_C - m_C$$

$$u_C = P_C U_{MC} \tanh\left(\frac{\alpha E(z)}{U_{MC}}\right)\beta_U C \quad \text{(Jassby and Platt, 1976)}$$

$$u_C = P_C U_{MC} \frac{E(z)}{\sqrt{E(z)^2 + (U_{MC}/\alpha)^2}}\beta_U C \quad \text{(Smith, 1936)}$$

$$\beta_U C = \tanh\left(s_C\left(\frac{P_N/P_C - NC_{min}}{NC_{max} - NC_{min}}\right)\right)$$

$$m_C = P_C m_{0C}. \qquad \text{(A1)}$$

In the uptake formulas, U_{MC} is the maximum growth rate, α the growth efficiency (initial slope of the photosynthesis curve), $E(z)$ the irradiance profile, β_{UC} a growth limiter as organisms approach NC_{min} and s_c the shape factor for the growth limiter ($s_c = 20$).

The growth limiter has no effect at moderate or high N:C. The basal metabolism rate is m_{0C}.

Cellular nitrogen (P_N, mg N cell^{-1})

Nitrogen uptake is based on Michaelis–Menten kinetics, again modified by a hyperbolic tangent limiter to slow uptake as the organisms approach their maximum N:C ratio (NC_{max}). Nitrogen excretion keeps cellular nitrogen from getting too large, but excretion only occurs at very high N:C ratios because of the hyperbolic tangent limiter. The limiter makes the model insensitive to changes in the nitrogen excretion rate, and is consistent with observations that nitrate excretion rates are typically less than 10% of uptake rates (Collos *et al.*, 2004).

$$\begin{aligned}
\frac{dP_N}{dt} &= \text{uptake} - \text{excretion} = u_N - e_N \\
u_N &= P_C U_{MN} \frac{\mathcal{N}(z)}{k_N + \mathcal{N}(z)} \beta_{UN}, \\
\beta_{UN} &= \tanh\left(-s_N\left(\frac{P_N/P_C - NC_{max}}{NC_{max} - NC_{min}}\right)\right) \\
e_N &= e_{Nmax} P_C \beta_{eN}, \\
\beta_{eN} &= \left(1 + \tanh\left(s_e \frac{P_N/P_C - NC_{max}}{NC_{max} - NC_{min}}\right)\right), \qquad \text{(A2)}
\end{aligned}$$

where U_{MN} is the maximum nitrogen uptake rate, k_N the half saturation constant, $\mathcal{N}(z)$ the nitrogen concentration profile, e_{Nmax} the maximum nitrogen excretion rate, β_{UN} a nitrogen uptake limiter as organisms approach NC_{max}, β_{eN} a nitrogen excretion limiter as organisms approach NC_{min} and s_N and s_e shape factors for the uptake and excretion limitation ($s_N = s_e = 20$).

Organisms per particle (P_A, cells)

The total number organisms in each particle is updated each time step. If cellular mass increases to the point that it is greater than or equal to the mass required for fission ($W_{fission}$), then the number of organisms in that particle doubles, and the carbon and nitrogen per cell are cut in half to conserve mass. Alternatively, if the cellular mass in a particle decreases below the minimum necessary for survival (W_{starve}), then the organisms in that particle die and the particle is removed from the model. Background mortality (Δ_0) decreases the number of organisms in each particle in proportion to its current population. Finally, if the number of organisms in a particle drops below 1, then the particle is removed from the model.

$$\begin{aligned}
\frac{dP_A}{dt} &= \Omega_{fission}(P_C, W_{fission}) - \Omega_{starvation}(P_C, W_{starve}) \\
&\quad - \Omega_{extinction}(P_A, 1) - \Delta_0 P_A \\
\text{fission}(\Omega_{fission}): &\quad P_A = 2P_A \text{ if } P_C > W_{fission} \\
\text{starvation}(\Omega_{starvation}): &\quad P_A = 0 \text{ if } P_C < W_{starve} \\
\text{extinction}(\Omega_{extinction}): &\quad P_A = 0 \text{ if } P_A < 1 \\
\text{mortality}: &\quad \Delta_0 P_A. \qquad \text{(A3)}
\end{aligned}$$

Swimming speed (w_s, m day^{-1})

Organism swimming speed is critical to vertical migration. Rather than diel phototaxis and geotaxis, the organisms in this model migrate based on their internal physiological state (Kamykowski and Yamazaki, 1997; Broekhuizen, 1999). Particles migrate up toward light at the surface at maximum swimming speed when their N:C ratio is within a given fraction (C_{up}) of the maximum N:C. Similarly, they swim down towards nutrients when N:C decreases to a fraction (C_{down}) of the minimum N:C. When the organisms have reached the nitracline, they hold position with zero swimming velocity as long as the ambient nitrogen concentration is large ($\mathcal{N} > 2k_N$). If turbulent fluctuations carry the particles either up or down away from the nitracline, the particles swim back toward the nitracline to resume nutrient uptake. After crossing a nutritional threshold (nitrogen replete or deficient), organisms continue with a swimming behavior until reaching the other threshold. An organism ascending toward the surface swims up until it becomes nitrogen deficient, and an organism at the nitracline holds position until is nitrogen replete.

$$\begin{aligned}
&\text{N replete}: w_s = +w_s \quad \text{if NC} > C_{up}(NC_{max} - NC_{min}) + NC_{min} \\
&\text{N deficient}: w_s = \begin{cases} -w_s & \text{if NC} < C_{down}(NC_{max} - NC_{min}) \\ & \quad + NC_{min} \text{ and } \mathcal{N} < 2k_N \\ 0 & \text{if NC} < C_{down}(NC_{max} - NC_{min}) \\ & \quad + NC_{min} \text{ and } \mathcal{N} > 2k_N \\ +w_s & \text{if NC} < C_{down}(NC_{max} - NC_{min}) \\ & \quad + NC_{min} \text{ and } \mathcal{N} > 4k_N \end{cases} \qquad \text{(A4)}
\end{aligned}$$

Particle advection/dispersion

The change in the position of each particle is the sum of a stochastic, turbulent displacement and a deterministic, advective component due to swimming or sinking. The dispersive, random walk displacement includes a deterministic term to account for non-uniformity in the turbulent diffusivity $K_z(z)$ (Visser, 1997; Ross and Sharples, 2004). The deterministic component keeps particles from artificially accumulating in regions of low turbulent diffusivity. Vertical position at the next time step (z_{n+1}) depends on the previous position (z_n), the deterministic and random components of turbulent displacement and advection due to swimming or sinking. The vertical advection speed (w_s) is the sum of swimming (w_{swim}) and sinking (w_{sink}) speeds, but for the model runs presented here $w_{sink} = 0$. R is a random number with uniform probability distribution between -1 and 1. The model time step is sufficiently small to meet the criterion implicit in equation (A5) that $K_z(z)$ is well-approximated by a first-order Taylor series expansion (Ross and Sharples, 2004).

$$z_{n+1} = z_n + \frac{\partial K_z(z_n)}{\partial z}\Delta t + R\left[\frac{2K_z(z_n + \frac{1}{2}\partial K_z(z_n)/\partial z \Delta t)\Delta t}{r}\right]^{1/2} + w_s \Delta t$$
$$R \in [-1, 1]$$
$$r = \mathrm{var}(R) = \frac{1}{3}. \qquad \text{(A5)}$$

Light profile (E, μmol photons m^{-2} s^{-1})

The light profile in the water column depends on the maximum daily irradiance (E_{0max}), the extinction coefficient (k_E) and the number of hours of light per day (T_{day}).

$$-E(z,t) = E_0(t)e^{-k_E z}$$
$$E_0(t) = E_{0max}\sin\left(\frac{t\pi}{T_{day}}\right) \quad \text{for} \quad 12 - \frac{T_{day}}{2} \le t \le 12 + \frac{T_{day}}{2}. \qquad \text{(A6)}$$

Turbulent diffusivity (K_z, m^2 s^{-1})

The turbulent diffusivity (K_z) sets the random component of particle advection, and is meant to represent transport by turbulent eddies. The diffusivity in the base simulation is scaled from observations on the New England shelf during April and May 1997 (MacKinnon and Gregg, 2005). Turbulent diffusivity depends on turbulent dissipation (ε) and stratification ($N^2 = -g/\rho_0(\partial\rho/\partial z)$): $K_z = \alpha\varepsilon N^2$, where $\alpha = 0.2$ (Osborn, 1980).

Turbulent dissipation is generated by wind stress at the surface, represented by the friction velocity at the surface: $u_* = \sqrt{\tau_w/\rho_0}$, where τ_w is the wind stress and $\rho_0 \sim 1000$ kg m^{-3} is the density of water. The friction velocity is parameterized based on the wind speed 10 m above the surface (U_{10}): $u_* = f_c\ U_{10}$, where $f_c = 0.00123$. Turbulent dissipation in the mixed layer decreases with depth according to $\varepsilon = 1.76u_*^3/\kappa z$, where $\kappa = 0.4$ is von Karman's constant, and the constant of 1.76 is based on observations (Lombardo and Gregg, 1989). Using this vertical profile for ε, the turbulent diffusivity profile is then $K_z = \alpha(f_c\ U_{10})^3/\kappa N^2 z$. The profile is smoothed near the surface by applying nearly constant K_z for $z <$ 2 m; this removes the singularity at $z = 0$ and makes $\partial K_z/\partial z(z = 0) \sim 0$ so that particles do not artificially collect at the surface boundary (Ross and Sharples, 2004).

REFERENCES

Anderson, D. M. and Stolzenbach, K. D. (1985) Selective retention of two dinoflagellates in a well-mixed estuarine embayment: the importance of diel vertical migration and surface avoidance. *Mar. Ecol. Prog. Ser.*, **25**, 39–50.

Anderson, D. M., Kulis, D. M. and Binder, B. J. (1984) Sexuality and cyst formation in the dinoflagellate *Gonyaulax tamarensis*: cyst yield in batch cultures. *J. Phycol.*, **20**, 418–425.

Anderson, D. M., Kulis, D. M., Sullivan, J. J. *et al.* (1990) Dynamics and physiology of saxitoxin production by the dinoflagellates *Alexandrium* spp. *Mar. Biol.*, **104**, 511–524.

Anderson, D. M., Kulis, D. M., Doucette, G. J. *et al.* (1994) Biogeography of toxic dinoflagellates in the genus *Alexandrium* from the northeastern United States and Canada. *Mar. Biol.*, **120**, 467–478.

Anderson, D. M., Townsend, D. W., McGillicuddy, D. J., Jr *et al.* (2005) The ecology and oceanography of toxic *Alexandrium fundyense* blooms in the Gulf of Maine. *Deep-Sea Res. Pt II*, **52**, 2365–2368.

Ault, T. R. (2000) Vertical migration by the marine dinoflagellate *Prorocentrum triestinum* maximizes photosynthetic yield. *Oecologia*, **125**, 466–475.

Barkmann, W. and Woods, J. D. (1996) On using a Lagrangian model to calibrate primary production determined from *in vitro* incubation measurements. *J. Plankton Res.*, **18**, 767–788.

Bauerfeind, E., Elbrachter, M., Steiner, R. *et al.* (1986) Application of laser doppler spectroscopy (LDS) in determining swimming velocities of motile phytoplankton. *Mar. Biol.*, **93**, 323–327.

Blasco, D. (1978) Observations on the diel migration of marine dinoflagellates off the Baja California coast. *Mar. Biol.*, **46**, 41–47.

Broekhuizen, N. (1999) Simulating motile algae using a mixed Eulerian-Lagrangian approach: does motility promote dinoflagellate persistence or co-existence with diatoms? *J. Plankton Res.*, **21**, 1191–1216.

Broekhuizen, N., Oldman, J. and Zeldis, J. (2003) Sub-grid-scale differences between individuals influence simulated phytoplankton production and biomass in a shelf-sea system. *Mar. Ecol. Prog. Ser.*, **252**, 61–76.

Cochlan, W. P., Harrison, P. J. and Denman, K. L. (1991) Diel periodicity of nitrogen uptake by marine phytoplankton in nitrate-rich environments. *Limnol. Oceanogr.*, **36**, 1689–1700.

Collos, Y., Gagne, C., Laabir, M. *et al.* (2004) Nitrogeneous nutrition of *Alexandrium catenella* (dinophyceae) in cultures in Thau Lagoon, Southern France. *J. Phycol.*, **40**, 96–103.

Collos, Y., Vaquer, A. and Souchu, P. (2005) Acclimation of nitrate uptake by phytoplankton to high substrate levels. *J. Phycol.*, **41**, 466–478.

Cullen, J. J. (1985) Diel vertical migration by dinoflagellates: roles of carbohydrate metabolism and behavioral flexibility. In Rankin, M. A. (ed.), *Migration: mechanisms and adaptive significance*. Univ. Texas *Contrib. Mar. Sci.*, 27, 135–152.

Cullen, J. J. and Horrigan, S. G. (1981) Effects of nitrate on the diurnal vertical migration, carbon to nitrogen ratio, and the photosynthetic capacity of the dinoflagellate. *Gymnodinium splendens*. *Mar. Biol.*, **62**, 81–89.

Cullen, J. J. and MacIntyre, J. G. (1998) Behavior, physiology, and the niche of depth-regulating phytoplankton. In Anderson, D. M, Cembella, A. D., and Hallegraeff, G. M. (ed.). *Physiological Ecology of Harmful Algal Blooms*. Springer-Verlag, Berlin, pp. 559–579.

Cullen, J. J., Stewart, E., Renger, E. *et al.* (1983) Vertical motion of the thermocline, nitracline and chlorophyll maximum layers in relation to currents on the Southern California Shelf. *J. Mar. Res.*, **41**, 239–262.

Denman, K. L. and Gargett, A. E. (1983) Time and space scales of vertical mixing and advection of phytoplankton in the upper ocean. *Limnol. Oceanogr.*, **28**, 801–815.

Eppley, R. W., Holm-Hansen, O. and Strickland, J. D. H. (1968) Some observations on the vertical migration of dinoflagellates. *J. Phycol.*, **4**, 333–340.

Fauchot, J. J., Levasseur, M. and Roy, S. (2005a) Daytime and nighttime vertical migrations of *Alexandrium tamarense* in the St. Lawrence estuary (Canada). *Mar. Ecol. Prog. Ser.*, **296**, 241–250.

Fauchot, J., Levasseur, M., Roy, S. *et al.* (2005b) Environmental factors controlling *Alexandrium tamarense* (dinophyceae) growth rate during a red tide event in the St. Lawrence estuary (Canada). *J. Phycol.*, **41**, 263–272.

Flynn, K. J. (2002) Toxin production in migrating dinoflagellates: a modeling study of PSP producing *Alexandrium*. *Harmful Algae*, **1**, 147–155.

Flynn, K. J. and Fasham, M. J. R. (2002) A modeling exploration of vertical migration by phytoplankton. *J. Theor. Biol.*, **218**, 471–484.

Flynn, K., Jones, K. J. and Flynn, K. J. (1996) Comparisons among species of *Alexandrium* (dinophyceae) grown in nitrogen- or phosphorus-limiting batch culture. *Mar. Biol.*, **126**, 9–18.

Franks, P. J. S. and Anderson, D. M. (1992) Alongshore transport of a toxic phytoplankton bloom in a buoyancy current: *Alexandrium tamarense* in the Gulf of Maine. *Mar. Biol.*, **112**, 153–164.

Garcés, E., Vila, M., Masó, M. *et al.* (2005) Taxon-specific analysis of growth and mortality rates of harmful dinoflagellates during bloom conditions. *Mar. Ecol. Prog. Ser.*, **301**, 67–79.

Geyer, W. R. and Ledwell, J. R. (1994) Final Report: Massachusetts Bay Dye Study. Massachusetts Water Resources Authority, Boston. Report ENQUAD 1994–17. 13 pp. + tables and figures.

Glibert, P. M., Anderson, D. M., Gentien, P. *et al.* (2005) The global, complex phenomena of harmful algal blooms. *Oceanography*, **18**, 136–147.

Heaney, S. I. and Eppley, R. W. (1981) Light, temperature and nitrogen and interacting factors affecting diel vertical migrations of dinoflagellates in culture. *J. Plankton Res*, **3**, 331–344.

Holligan, P. M., Balch, W. M. and Yentsch, C. M. (1984) The significance of subsurface chlorophyll, nitrate and ammonium maxima in relation to nitrogen for phytoplankton growth in stratified waters of the Gulf of Maine. *J. Marine Res.*, **42**, 1051–1073.

Jassby, A. D. and Platt, T. (1976) Mathematical formulation of the relationship between photosynthesis and light for phytoplankton. *Limnol. Oceanogr.*, **21**, 540–547.

John, E. H. and Flynn, K. J. (2002) Modelling changes in paralytic shellfish toxin content of dinoflagellates in response to nitrogen and phosphorous supply. *Mar. Ecol. Prog. Ser.*, **225**, 147–160.

Kamykowski, D. (1995) Trajectories of autotrophic marine dinoflagellates. *J. Phycol.*, **31**, 200–208.

Kamykowski, D. and McCollum, S. A. (1986) The temperature acclimated swimming speed of selected marine dinoflagellates. *J. Plankton Res.*, **8**, 275–287.

Kamykowski, D. and Yamazaki, H. (1997) A study of metabolism-influenced orientation in the diel vertical migration of marine dinoflagellates. *Limnol. Oceanogr.*, **42**, 1189–1202.

Kamykowski, D., Reed, R. E. and Kirkpatrick, G. J. (1992) Comparison of sinking velocity, swimming velocity, rotation and path characteristics among six marine dinoflagellate species. *Mar. Biol.*, **113**, 319–328.

Kudela, R. M., Cochlan, W. P. and Dugdale, R. C. (1997) Carbon and nitrogen uptake response to light by phytoplankton during an upwelling event. *J. Plankton Res.*, **19**, 609–630.

Lombardo, C. and Gregg, M. (1989) Similarity scaling of viscous an thermal dissipation in a convecting surface boundary layer. *J. Geophys. Res.*, **94**, 6273–6284.

Love, R. C., Loder, T. C., III and Keafer, B. A. (2005) The ecology and oceanography of toxic *Alexandrium fundyense* blooms in the Gulf of Maine. *Deep-Sea Res. Pt II*, **52**, 2450–2466.

MacIsaac, J. J. (1978) Diel cycles of inorganic nitrogen uptake in a natural phytoplankton population dominated by. *Gonyaulax polyedra*. *Limnol. Oceanogr.*, **23**, 1–9.

MacIsaac, J. J., Grunseich, G. S., Glover, H. E. *et al.* (1979) Light and nutrient limitation in *Gonyaulax excavate*: nitrogen and carbon trace results. In Taylor, D. L. and Seliger, H. H. (eds), *Toxic Dinoflagellate Blooms*. Elsevier North Holland, New York, pp. 107–110.

MacIntyre, J. G., Cullen, J. J. and Cembella, A. D. (1997) Vertical migration, nutrition and toxicity in the dinoflagellate *Alexandrium tamarense*. *Mar. Ecol. Prog. Ser.*, **148**, 201–216.

MacKinnon, J. A. and Gregg, M. C. (2005) Spring mixing: turbulence and internal waves during restratification on the New England shelf. *J. Phys. Oceanogr.*, **35**, 2425–2443.

McGillicuddy, D. J. (1995) One dimensional numerical simulation of new primary production: Lagrangian and Eulerian formulations. *J. Plankton Res.*, **17**, 405–412.

McGillicuddy, D. J., Signell, R. P., Stock, C. A. *et al.* (2003) A mechanism for offshore initiation of harmful algal blooms in the coastal Gulf of Maine. *J. Plankton Res.*, **25**, 1131–1138.

McGillicuddy, D. J., Anderson, D. M., Lynch, D. R. *et al.* (2005) Mechanisms regulating large-scale seasonal fluctuations in *Alexandrium fundyense* populations in the Gulf of Maine: results from a physical–biological model. *Deep-Sea Res. Pt II*, **52**, 2698–2714.

Osborn, T. R. (1980) Estimates of the local rate of vertical diffusion from dissipation measurements. *J. Phys. Oceanogr.*, **10**, 83–89.

Passow, U. (1991) Vertical migration of *Gonyaulax catenata* and *Mesodinium rubrum*. *Mar. Biol.*, **110**, 455–463.

Peters, F. and Marrasé, C. (2000) Effects of turbulence on plankton: an overview of experimental evidence and some theoretical considerations. *Mar. Ecol. Prog. Ser.*, **205**, 291–306.

Rasmussen, J. and Richardson, K. (1989) Response of *Gonyaulax tamarensis* to the presence of a pycnocline in an artificial water column. *J. Plankton Res.*, **11**, 747–762.

Richardson, T. L., Cullen, J. J., Kelley, D. E. *et al.* (1998) Potential contributions of vertically migrating *Rhizosolenia* to nutrient cycling and new production in the open ocean. *J. Plankton Res.*, **20**, 219–241.

Ross, O. N. and Sharples, J. (2004) Recipe for 1-D Lagrangian particle tracking models in space-varying diffusivity. *Limnol. Oceanogr.-Meth.*, **2**, 289–302.

Smayda, T. J. (1997) Harmful algal blooms: their ecophysiology and general relevance to phytoplankton blooms in the sea. *Limnol. Oceanogr.*, **42**, 1137–1153.

Smith, E. L. (1936) Photosynthesis in relation to light and carbon dioxide. *Proc. Natl. Acad. Sci. Wash.*, **22**, 504–511.

Stock, C. A., McGillicuddy, D. J., Solow, A. R. *et al.* (2005) Evaluating hypotheses for the initiation and development of *Alexandrium fundyense* blooms in the western Gulf of Maine using a coupled physical–biological model. *Deep-Sea Res. Pt II*, **52**, 2715–2744.

Sullivan, J. M., Swift, E., Donaghay, P. L. *et al.* (2003) Small-scale turbulence affects the division rate and morphology of two red-tide dinoflagellates. *Harmful Algae*, **2**, 183–199.

Tett, P. and Droop, M. R. (1988) Cell quota models and planktonic primary production. In Wimpenny, J. W. T. (ed.), *CRC Handbook of Laboratory Model Systems for Microbial Ecosystems*. CRC Press, Boca Raton, FL, pp. 177–233.

Townsend, D. W., Pettigrew, N. R. and Thomas, A. C. (2001) Offshore blooms of the red tide dinoflagellate, *Alexandrium* sp., in the Gulf of Maine. *Cont. Shelf Res.*, **21**, 347–369.

Townsend, D. W., Bennett, S. L. and Thomas, M. A. (2005a) Diel vertical distributions of the red tide dinoflagellate *Alexandrium fundyense* in the Gulf of Maine. *Deep-Sea Res. Pt II*, **52**, 2593–2602.

Townsend, D. W., Pettigrew, N. R. and Thomas, A. C. (2005b) On the nature of *Alexandrium fundyense* blooms in the Gulf of Maine. *Deep-Sea Res. Pt II*, **52**, 2603–2630.

Villareal, T. A., Altabet, M. A. and Culver-Rymsza, K. (1993) Nitrogen transport by vertically migrating diatom mats in the North Pacific Ocean. *Nature*, **363**, 709–712.

Visser, A. W. (1997) Using random walk models to simulate the vertical distribution of particles in a turbulent water column. *Mar. Ecol. Prog. Ser.*, **158**, 275–281.

White, A. E., Spitz, Y. H., Karl, D. M. *et al.* (2006) Flexible elemental stoichiometry in *Trichodesmium* spp. and its ecological implications. *Limnol. Oceanogr.*, **51**, 1777–1790.

Woods, J. and Barkmann, W. (1994) Simulating Plankton Ecosystems by the Lagrangian Ensemble Method. *Philos. Trans. R. Soc. Lond. B Biol. Sci.*, **343**, 27–31.

Yamamoto, T., Seike, T., Hashimoto, T. *et al.* (2002) Modelling the population dynamics o the toxic dinoflagellate *Alexandrium tamarense* in Hiroshima Bay, Japan. *J. Plankton Res.*, **24**, 33–47.